International Journal of Materials Science and Technology Studies
ISSN: 3006-7693 (Print), ISSN: 3006-3744 (Online) | Volume 5, Number 1, Year 2026
DOI: https://doi.org/10.62051/ijmsts.v5n1.01
Journal homepage: https://wepub.org/index.php/IJMSTS/index

Influence of Setting Accelerator Dosage on Fresh Properties, Strength Development and Microstructure of Ultrafine Silicate Cement Grout

Bofang Zhou [1, *], Xiangrui Meng [1], Yanfen Wang [2]

[1] School of Mining Engineering, Anhui University of Science and Technology, Huainan, Anhui Province, 232001, China

[2] School of Materials Science and Engineering, Anhui University of Science and Technology, Huainan, Anhui 232001, China

*Corresponding Author

ABSTRACT

As mining depth increases, roadway surrounding rock in underground coal mines is increasingly prone to severe deformation and failure. In particular, the mechanical behaviour of weak, soft rock masses is highly heterogeneous and difficult to control, making reliable stability management challenging. Grouting reinforcement has therefore become an effective intervention for improving the integrity and load-bearing capacity of the surrounding rock. With the growing complexity of engineering–geological conditions, grouting materials are required to deliver rapid setting and early strength while maintaining anti-dispersion performance and long-term durability. To meet the demand for fast solidification and efficient support under deep-mine conditions, this study develops an ultrafine silicate cement–based grout incorporating an expansive agent (8%), a water-reducing agent (0.35%) and a setting accelerator (1.0–3.5%), with the water-to-cement ratio fixed at 0.40. Using a suite of macro- and micro-scale characterization methods, we quantify how accelerator dosage governs slurry workability, mechanical performance and the microstructure of hardened grout, and we elucidate the associated hydration mechanisms. Increasing accelerator content markedly shortened the setting time by 61.54–97.50% (relative to the control) but reduced flowability, whereas both compressive and flexural strengths exhibited a non-monotonic trend, increasing initially and then declining at higher dosages. An accelerator dosage of 2.5% yielded the best overall performance, increasing 3-day compressive and flexural strengths by 14.40% and 125.12%, respectively, and improving 28-day compressive strength by 14.76%. Microstructural evidence further indicates that an appropriate accelerator dosage promotes a denser and more homogeneous hydration-product network, thereby enhancing structural stability. Overall, maintaining the accelerator dosage within 2.0–2.5% provides an optimal balance between setting kinetics and mechanical capacity, and is therefore well suited for grouting applications in high-stress deep-coal environments.

KEYWORDS

Ultrafine silicate cement; Accelerator; Grouting material; Setting time

1. INTRODUCTION

As coal extraction continues, mines are progressively extending to greater depths, where deep coal operations commonly contend with high in-situ stress, elevated geothermal conditions, high gas content, and complex hydrogeology. These coupled factors degrade surrounding-rock stability and exacerbate geohazards such as water–mud inrush, posing persistent threats to safe production [1].

Grouting reinforcement is a widely adopted and effective measure for geohazard prevention and control, with established applications in roadway support, water inrush mitigation, and strata consolidation in coal mines [2]. For rapid sealing and timely support in deep, heterogeneous formations, grouting materials must combine adequate injectability with reliable strength development, while also providing controllable early-age setting to shorten construction time and improve reinforcement efficiency [3]. Ultrafine silicate cement, characterized by a small particle size, large specific surface area, and high hydration reactivity, offers superior penetrability and strength gain, and has therefore become a preferred inorganic binder for coal-mine grouting [4]. However, its setting and hardening can remain insufficiently rapid for emergency scenarios requiring immediate water-source cut-off and prompt stabilization of surrounding rock. Setting accelerators [5], as common admixtures, can regulate hydration kinetics to markedly accelerate setting and hardening and enhance early strength, thereby offering substantial engineering value. Although the effects of accelerators on ordinary Portland cement have been investigated [6]-[10]—for example, Zhang et al. [11] reported that alkali-free accelerators promote the formation of hydration products such as AFt and C–S–H to improve early strength, yet may reduce later-age strength—and Cha et al. [12] identified an optimal dosage range for combined accelerator and water reducer in CGS systems, noting that excessive accelerator compromises strength. Nevertheless, for ultrafine silicate cement—particularly under fixed expansive-agent and water-reducer conditions—systematic understanding of how accelerator dosage governs slurry performance and mixture suitability remains limited, and the synergistic optimization of setting rate and mechanical performance under deep-mine service conditions warrants further investigation.

Accordingly, this study employs ultrafine silicate cement as the primary binder, with an expansive agent fixed at 8% and a water-reducing agent fixed at 0.35%, at a constant water-to-cement ratio of 0.40. The dosage of setting accelerator (1.0%, 1.5%, 2.0%, 2.5%, 3.0%, and 3.5%) is taken as the key variable in a systematic experimental program. Setting time, flowability, compressive strength, and flexural strength are quantified across mixtures, and microstructural characterization is used to elucidate the underlying mechanisms and delineate an appropriate dosage window. The findings are intended to provide both theoretical basis and practical guidance for rapid solidification and engineering adaptation of grouting materials in high-stress, high-permeability surrounding rock environments in deep coal mines.

2. MATERIALS AND EXPERIMENTAL METHODS

2.1. Materials

Ultrafine cement (K1340) was supplied by Shandong Kangjing New Materials Technology Co., Ltd. It is a Grade I ultrafine silicate cement, and its chemical composition is shown in Figure 1. The admixtures included a polycarboxylate-based water-reducing agent (bulk density: 500 ± 0.02 g/L; solid content > 98%), an expansive agent produced by Henan Mingzhu Chemical Co., Ltd. (main component: CaO; mass fraction: 70.80%), and a J85-type setting accelerator supplied by Huaibei Xinda New Building Materials Co., Ltd. Photographs of the raw materials are provided in Figure 2.

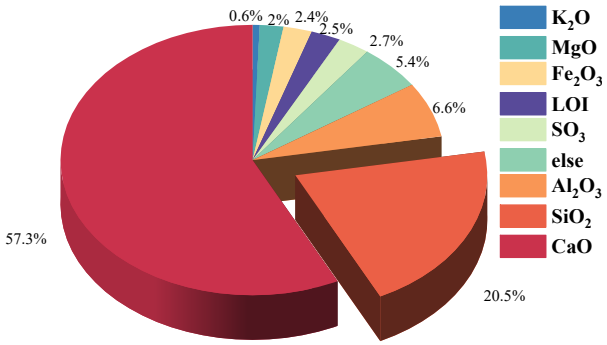

Figure 1. Composition of ultrafine silica cement (weight percentage)

Figure 2. Required Raw Materials

2.2. Proportioning and Sample Preparation

A single-factor experimental program was designed according to Table 1. Predetermined amounts of ultrafine silicate cement, setting accelerator, expansive agent, and water-reducing agent were weighed and introduced into a powder mixer for dry blending for 5 min. An appropriate amount of water was then added, followed by high-speed mixing for 120 s until a homogeneous slurry free of visible sediment was obtained, yielding the ultrafine silicate cement–based grouting material.

The prepared composite slurry was cast into prismatic moulds (40 mm × 40 mm × 160 mm). After vibration compaction and surface finishing, the specimens were stored in a curing chamber for 24 h and then demoulded. Curing was subsequently conducted under standard conditions (20 ± 2 °C, 99% relative humidity) to designated ages of 3 d (±45 min), 7 d (±2 h), and 28 d (±8 h).

Table 1. Mix proportions of grout specimens (by mass)

Sample	Cement	Accelerator	Expansive agent	Water reducer	Water
B1	100	1	8	0.35	40
B2	100	1.5	8	0.35	40
B3	100	2	8	0.35	40
B4	100	2.5	8	0.35	40
B5	100	3	8	0.35	40
B6	100	3.5	8	0.35	40

2.3. Experimental Methods

The mechanical properties of the hardened grout at specified curing ages were evaluated. Flexural strength was first measured using a cement electric flexural testing machine (DKZ-5000, Xiyi Building Materials Instrument Factory; maximum capacity: 11.5 MPa), followed by compressive strength testing using an automatic constant-stress testing machine (YES-300, Shanghai Yingsong Industrial and Mining Equipment Instrument Co., Ltd.; maximum load: 300 kN) at a loading rate of 0.5 kN/s.

Setting time was determined using a Vicat apparatus in accordance with *Test Methods for Water Requirement of Normal Consistency, Setting Time and Soundness of the Portland Cement Paste* (GB/T 1346-2011). Bleeding was quantified by pouring 100 mL of fresh grout into a graduated cylinder and allowing it to stand for 30 min; the scale corresponding to the interface between the supernatant water and the underlying slurry was recorded, and the bleeding rate was calculated accordingly. Flowability was measured using a truncated-cone mould (60 mm × 70 mm × 100 mm; height × top inner diameter × bottom inner diameter). The mould was filled with grout and levelled flush with the rim, then lifted vertically and steadily to allow the slurry to spread freely without disturbance until cessation; the diameter of the resulting spread circle was measured and taken as the flowability.

Phase assemblages of the hardened specimens were characterized by X-ray diffraction (XRD) using Cu Kα radiation (λ = 1.54060 Å) at a scanning rate of 5°/min. Microstructural features were examined by scanning electron microscopy (SEM). Surface functional groups were analyzed by Fourier transform infrared spectroscopy (FTIR) over 500–4000 cm^{-1} with an acquisition time of 30 s and a spectral resolution of 2 cm^{-1}.

3. RESULTS AND DISCUSSION

3.1. Grout Properties

Setting time is one of the key indicators used to evaluate the workability of grouting materials [13]. Figure 3 presents the setting times of ultrafine silicate cement grout as a function of accelerator dosage. Specimen B1 exhibited an initial setting time of 200 min and a final setting time of 326 min, whereas B2 showed 166 min and 227 min, respectively. Further increasing the accelerator content led to a pronounced reduction in setting time: B3 (84/144 min), B4 (24/63 min), B5 (13/46 min), and B6 (5/15 min) for initial/final setting. Overall, both initial and final setting times decreased sharply with increasing accelerator dosage. This behavior can be attributed to the accelerator supplying abundant Al^{3+} and SO_4^{2-} species as well as heterogeneous nucleation sites, which rapidly participate in reactions with C_3A, $CaSO_4 \cdot 2H_2O$, and water in the cement system. As a result, large quantities of acicular/rod-like ettringite (AFt) precipitate quickly on cement particle surfaces and grow in an interlaced, bridging manner between particles, forming a rigid percolated framework that effectively "locks" the slurry and accelerates the transition from a fluid to a solid-like state, thereby markedly shortening both initial and final setting times. At higher dosages, the increased availability of reactive ions and nucleation sites further accelerates AFt precipitation and network formation, leading to progressively shorter setting times [14].

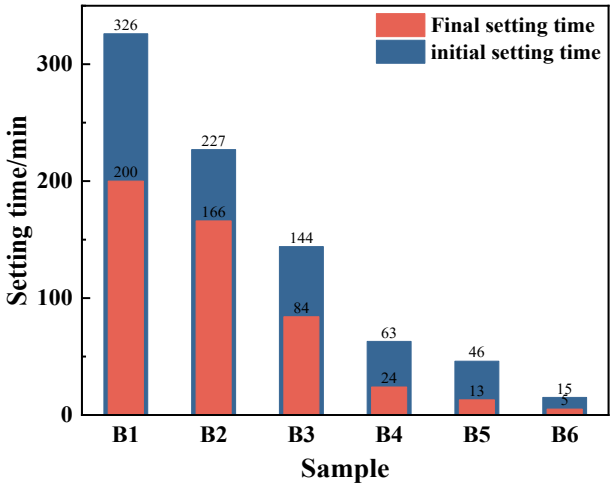

Figure 3. Setting time of slurry under different accelerator dosages

Figure 4 shows the bleeding behavior of the ultrafine silicate cement grout at different accelerator dosages. After casting the freshly mixed slurry into a graduated cylinder and allowing it to stand for 30 min, the measured bleeding rate was nearly zero for all mixtures, indicating excellent stability regardless of accelerator content. This can be attributed primarily to the ultrafine cement particles, which possess a small particle size and high specific surface area, thereby providing abundant adsorption sites that immobilize free water. In addition, the combined action of the setting accelerator and expansive agent promotes the rapid formation of hydration products such as ettringite (AFt) and C–S–H, which build an early skeletal framework that further constrains pore water and suppresses segregation. Consequently, the grout system behaves as a stable slurry with negligible bleeding within the tested time window [15].

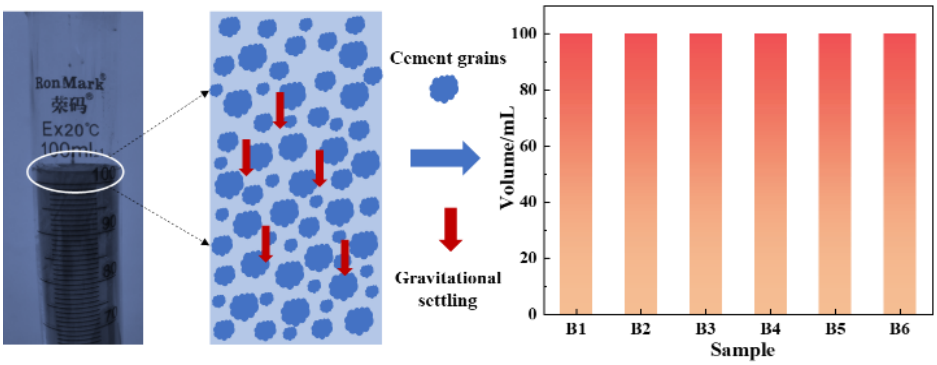

Figure 4. Bleeding rate under different accelerator dosages

Good flowability facilitates the penetration of grout into fractures and pores within broken surrounding rock. Figure 5 summarizes the spread diameters of ultrafine silicate cement grouts with different accelerator dosages. The measured flowability values for B1–B6 were 307 mm, 286.5 mm, 267.25 mm, 263.25 mm, 218.25 mm, and 184.5 mm, respectively. Overall, flowability increased progressively as the accelerator dosage decreased, indicating that higher accelerator contents significantly impair slurry workability. This reduction in flowability at high dosages (≥2.5%) is primarily attributed to the strong affinity of Al^{3+}/SO_4^{2-} species released from the accelerator for the ultrafine cement particle surfaces. Such species can dominate adsorption sites and compress the electrical double layer, thereby undermining the steric stabilization provided by the polycarboxylate superplasticizer through competitive adsorption and reduced electrostatic/steric repulsion. The resulting particle flocculation increases water entrapment within agglomerates and lowers the amount of effective free water, leading to a higher apparent viscosity and reduced spread. In parallel, at elevated dosages the accelerator can act synergistically with the expansive agent to trigger rapid, abundant precipitation of ettringite (AFt), which accelerates hydration and promotes premature structural build-up, further increasing flow resistance [16]. As the accelerator dosage is lowered, the dispersing efficiency of the water reducer is gradually restored, flocculated structures are disrupted, previously immobilized water is released, AFt precipitation is moderated, and particle dispersion improves—collectively increasing the effective free-water availability and reducing slurry flow resistance.

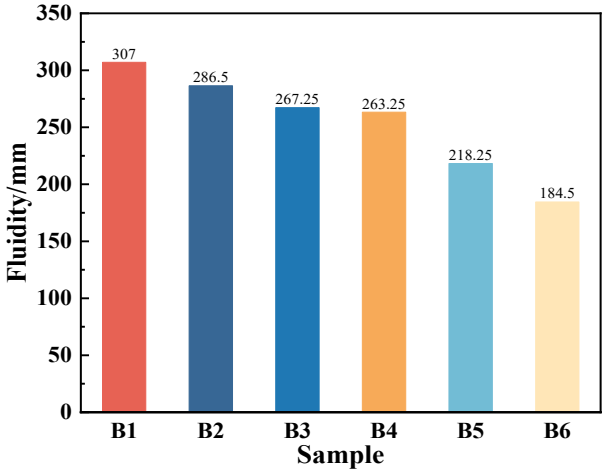

Figure 5. The fluidity of slurry under different accelerators

3.2. Mechanical Properties

Figure 6(a) presents the compressive strength of hardened ultrafine silicate cement grout at different curing ages as a function of accelerator dosage, and Fig. 6(b) provides a three-dimensional mapping of compressive strength versus accelerator dosage and curing time. As shown, the strength contours display a clear "peak-centered" distribution, with the highest compressive strength occurring at an accelerator dosage of 2.5% at 28 d, and progressively lower strengths radiating outward from this optimum. Overall, the compressive strength exhibits a non-monotonic dependence on accelerator dosage: as the dosage decreases, strength first increases and then declines.When the accelerator dosage is excessive (e.g., B6 at 3.5%), overly rapid setting can induce premature surface hardening of cement particles, forming a dense "shell" that restricts subsequent water ingress and limits continued hydration of the particle core. This self-inhibition of hydration constrains later-age microstructural development and, consequently, strength gain. Conversely, at an insufficient dosage (e.g., B1 at 1.0%), the accelerator provides inadequate kinetic stimulation; setting and hardening proceed too slowly to establish an effective early load-bearing skeleton, resulting in suboptimal compressive strength. Within an appropriate dosage window, the accelerator promotes early solidification while still permitting sustained and stable hydration at later ages, thereby enabling the grout to develop comparatively higher compressive strength.

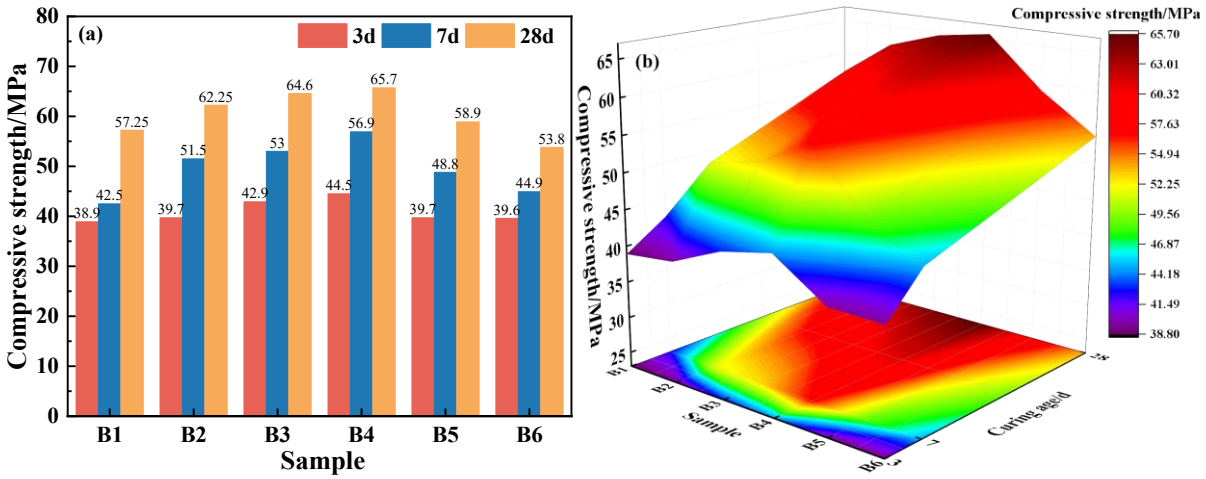

Figure 6. (a) the compressive strength of the stone body, (b) the three-dimensional mapping of the compressive strength with the dosage of the accelerator and the curing age

Figure 7(a) shows the flexural strength of hardened ultrafine silicate cement grout at different curing ages under varying accelerator dosages, and Fig. 7(b) presents the corresponding three-dimensional

response surface with respect to accelerator dosage and curing time. The contour distribution on the projected plane follows a pattern broadly consistent with that of compressive strength. At high accelerator dosages, the slurry undergoes very rapid setting, which tends to introduce more structural discontinuities and defects; under bending, these defects act as preferential stress concentrators that facilitate crack initiation and propagation, thereby reducing flexural strength. At low dosages, by contrast, the early-age skeleton develops slowly and remains comparatively porous and weakly connected, again making the material susceptible to stress localization and crack growth. With an appropriate accelerator dosage, the hydration process is better balanced, yielding a more continuous and uniformly distributed load-bearing framework with fewer critical defects. This improves stress transfer and promotes more effective stress redistribution under bending, resulting in higher flexural strength. Notably, the highest flexural strength is observed at 7 d. This can be explained by the rapid reaction of active components in the accelerator with gypsum in the cement system, which diminishes the retarding effect of gypsum on C_3A. Consequently, C_3A hydrates intensively at early ages, producing abundant early hydration products such as ettringite (AFt). The associated rapid heat release accelerates setting and hardening, enabling a load-bearing skeleton to form quickly and thereby leading to a pronounced enhancement in 7 d flexural strength.

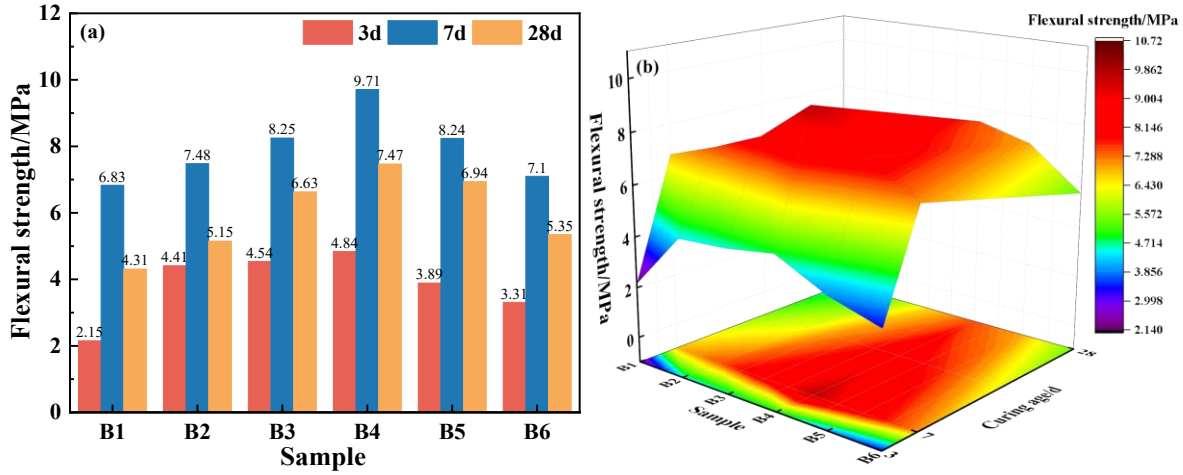

Figure 7. (a) Three-dimensional mapping of flexural strength of stone body, (b) Three-dimensional mapping of flexural strength with accelerator content and curing age

3.3. Microscopic Characteristics

Figure 8 shows the XRD patterns of hardened ultrafine silicate cement grouts cured for 28 d at different accelerator dosages. The dominant hydration products are C–S–H, portlandite (CH), and ettringite (AFt). Diffraction peaks associated with residual clinker phases (C_2S and C_3S), originating from unhydrated cement particles, are markedly weaker in mixture B4, suggesting more extensive hydration at an appropriate accelerator dosage. Monosulfate (AFm) [17], which forms via the conversion of AFt through reaction with C_3A, is also detected. The presence of $CaCO_3$ is mainly attributed to surface carbonation of $Ca(OH)_2$ during curing exposure to air. In addition, hemicarbonate (Hc) [18] and monocarbonate (Mc) [19] are identified, arising from the chemical reaction between C_3A-bearing aluminate phases and $CaCO_3$. When the availability of CO_3^{2-} is limited, Hc preferentially forms; as hydration proceeds and carbonate availability increases, part of Hc progressively transforms into Mc, which is conducive to microstructural refinement and densification of the hardened grout.

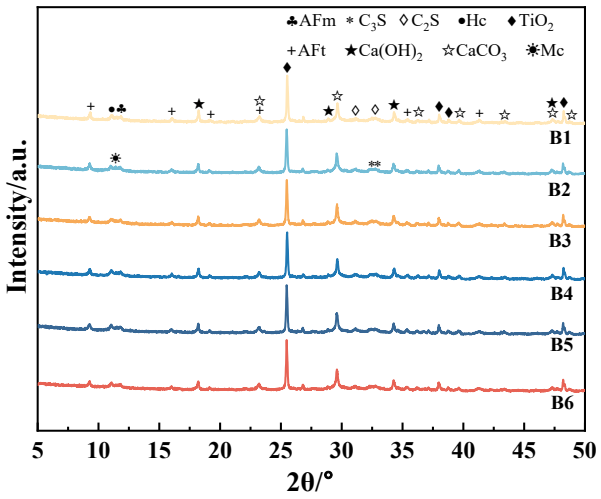

Figure 8. XRD pattern of the stone body of ultrafine portland cement grouting material

Figure 9 presents the FTIR spectra of hardened ultrafine silicate cement grouts cured for 28 d with different accelerator dosages. The band at ~532 cm^{-1} is dominated by Si–O vibrations and can be attributed to residual, unhydrated clinker phases (C_3S and C_2S). The Si–O–Si bending vibration at ~466 cm^{-1} and the Si–O stretching vibration at ~973 cm^{-1} are characteristic of the C–S–H gel. The peak at ~1126 cm^{-1} corresponds to S–O stretching vibrations of SO_4^{2-}, which primarily originate from ettringite (AFt). The sharp band at ~3643 cm^{-1} is assigned to the O–H stretching mode of portlandite (CH). In addition, the bands at ~3457 cm^{-1} and ~1650 cm^{-1} are associated with H–O–H vibrations of physically bound/free water, whereas the peaks at ~1432 cm^{-1} and ~875 cm^{-1} arise from CO_3^{2-} vibrations in $CaCO_3$ [20]. With increasing accelerator dosage, the sulfate-related (S–O) band intensifies markedly, indicating an increased abundance of AFt. Notably, the spectra of B3 and B4 exhibit sharper and better-resolved features, suggesting a more homogeneous hydration structure and more extensive formation of amorphous C–S–H within these mixtures.

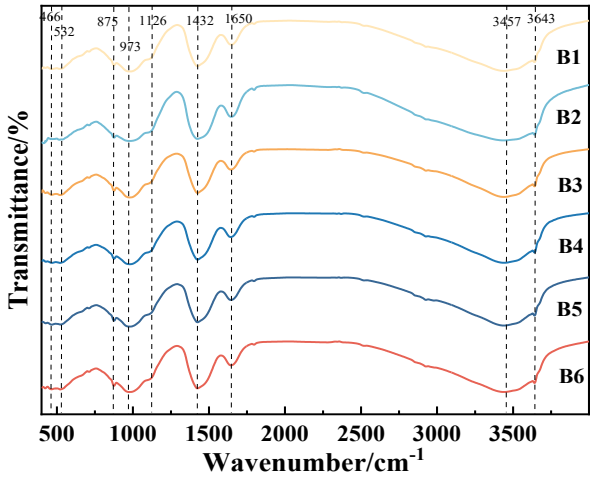

Figure 9. FTIR Spectrum of the Solidified Body of Ultrafine Silicate Cement Grouting Material

Figure 10 shows SEM micrographs of hardened ultrafine silicate cement grouts cured for 28 d with different accelerator dosages. All six specimens contain abundant hydration products, including plate-like portlandite (CH), acicular ettringite (AFt), and amorphous C–S–H gel. These phases intergrow and interlock to form a complex three-dimensional network; however, pronounced differences are observed in pore size distribution and overall compactness among the mixtures. In general, the matrix densification exhibits a non-monotonic dependence on accelerator dosage, increasing initially as the dosage decreases and then deteriorating at lower dosages. At either an insufficient or an excessive accelerator dosage (B1 and B6), the hardened matrix appears notably porous and poorly consolidated, with numerous pores of varying sizes, including elongated and partially interconnected voids. Such

a percolating pore structure is detrimental to mechanical performance because it reduces the effective load-bearing area and facilitates crack initiation and coalescence. By contrast, at intermediate dosages, a denser microstructure is evident: greater amounts of CH plates, AFt needles, and C–S–H gel are observed to bridge and entangle with one another, filling interparticle spaces and refining the pore network. The reduced porosity and improved continuity of the hydration-product framework provide a more stable microstructural basis for strength development in the hardened grout.

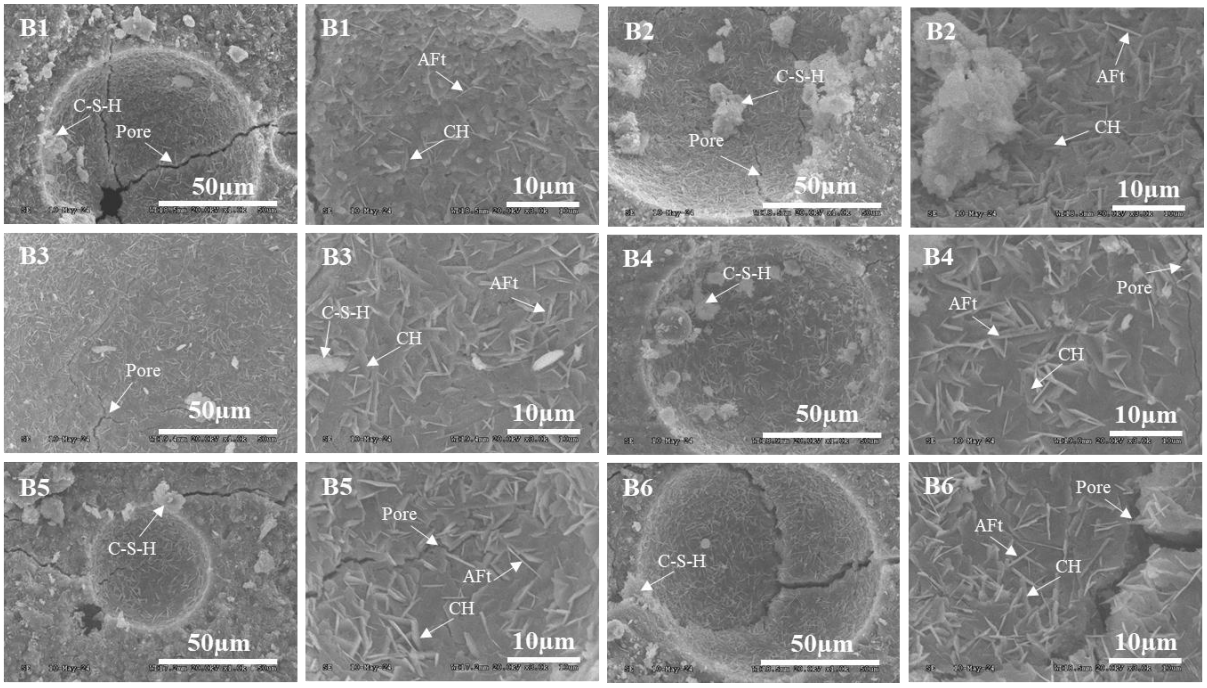

Figure 10. Ultrafine Portland cement grouting material stone body curing 28 days SEM pictures

3.4. Mechanism Analysis

Figure 11 schematically summarizes the hydration mechanisms of ultrafine silicate cement grout as regulated by accelerator dosage. The Al^{3+} and SO_4^{2-} species supplied by the accelerator promote rapid hydration of C_3S to form C–S–H, and simultaneously react with C_3A to generate substantial amounts of ettringite (AFt). These effects shorten the induction period [21] and accelerate the overall hydration kinetics, enabling the grout to transition more rapidly from a fluid to a solid-like state and thereby reducing the available flow window. Importantly, an appropriate accelerator dosage is required to maintain sufficient workability for injection while achieving timely setting [22]. As illustrated, when the accelerator dosage is within 2.0–2.5%, the availability of Al^{3+}/SO_4^{2-} is adequate to sustain an elevated hydration rate while maintaining a balanced formation of C–S–H and AFt. In this regime, densely intergrown C–S–H effectively fills interparticle spaces, and AFt needles are more uniformly distributed, leading to marked pore refinement and more homogeneous pore filling. The resulting compact microstructure provides a robust basis for improved overall performance of the grout. By contrast, at excessive dosages (3.0–3.5%), the high Al^{3+}/SO_4^{2-} supply drives an intense early reaction with C_3A and rapid AFt precipitation, which increases early hydration but can induce a pronounced "encapsulation effect" as fast-deposited products coat particle surfaces. This premature product layer may hinder continued hydration at later ages and can introduce internal structural stresses. Conversely, at low dosages (1.0–1.5%), the reduced concentration of Al^{3+}/SO_4^{2-} weakens kinetic activation, resulting in a lower degree of hydration, fewer hydration products, a coarser pore structure with higher porosity, and a less consolidated matrix, which is unfavorable for strength development.

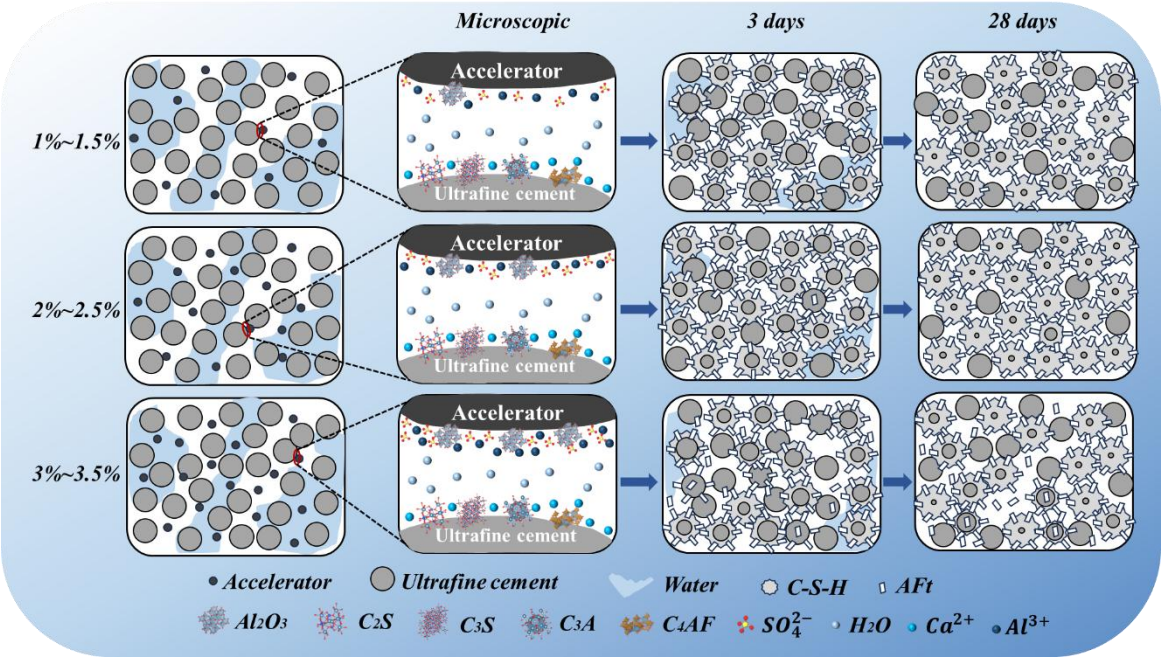

Figure 11. Hydration mechanism of ultrafine silicate cement grouting material under different accelerator dosages

4. CONCLUSIONS

(1) The setting behaviour and flowability of the ultrafine silicate cement grout are strongly governed by accelerator dosage, with both parameters decreasing monotonically as the accelerator content increases. At an accelerator dosage of 2.5%, the grout exhibits an initial and final setting time of 24 min and 63 min, respectively, with no visually detectable bleeding. These results demonstrate that the workability window and setting kinetics can be effectively tuned through dosage control.

(2) Incorporating an appropriate amount of accelerator enhances the mechanical performance of the grout. Both compressive strength and later-age flexural strength show a non-monotonic dependence on accelerator dosage, increasing initially as the dosage decreases and then declining at lower dosages. The optimal performance is achieved at 2.5% accelerator, at which the hardened grout attains a 3 d compressive strength of 44.50 MPa and a 7 d flexural strength of 6.47 MPa, demonstrating pronounced early-strength development; the 28 d compressive strength further reaches 65.7 MPa.

(3) XRD, FTIR and SEM analyses confirm that the principal hydration products are C–S–H gel, portlandite (CH), and ettringite (AFt). With increasing accelerator dosage, the pore structure of the hardened grout evolves in a non-monotonic manner, with pore prevalence and characteristic pore size decreasing initially and then increasing at higher dosages. At 2.5% accelerator, hydration products interlock more tightly, yielding finer pores and a markedly denser microstructure. Mechanistically, an optimal accelerator dosage accelerates hydration to generate sufficient reaction products while avoiding premature product accumulation, thereby producing a compact microstructure that underpins the overall performance improvement of the grout.

REFERENCES

[1] LI Jie. Evolution mechanism of wave velocity and mechanical properties in coal samples under water-satur-ated and cyclic stress coupling effects [J]. Safety in Coal Mines, 2025, 56(7): 98-106.

[2] SUN Yue, QIU Xincai, ZHANG Jinlei, et al. Experimental methods and reformation mechanism of grouting reinforcement infractured coal and rock masses [J]. Journal of Mine Automation, 2025, 51(06): 150-156.

[3] Wang Xueyun. Diffusion mode and curing effect of water glass in original loess under pressurized conditions [J]. Railway Engineering, 2025, 65(05): 129-135.

[4] WAN Xing. Performance characteristics and reinforcement effect of ultrafine cement grouting material [D]. Hunan: Hunan univer-sity of science and technology, 2022: 9-23.

[5] Yuan LAN, Xu Jie. Shotcrete and Accelerator: The "Golden Pair" in Construction Engineering [J]. Concrete World, 2025, (06): 9-11.

[6] Liu Jun. Study on Grouting Diffusion Mechanism and Engineering Application of Quick-setting Slurry in High Temperature Water-rich Fractured Rock Mass [D]. Jinan: Shandong University, 2023: 40-44.

[7] Zhu Daohe. Study on the modification and plugging characteristics of rapid setting of rich-water grouting materials [D]. Jiaozuo: Henan Polytechnic University, 2023: 42-48.

[8] Xie Bo, Shao Jinpeng, Gao Bo, et al. Analysis on Mechanism of Reinforcement of Water - rich Fractured Zone by Means of Grouting with New Type of Accelerator [J]. Tunnel construction, 2015, 35(4): 303-310.

[9] Guo Xianqiang, Huang Bin, Wang Yalei, et al. Research and Application of Rapid Setting Slurry Grouting Technology [J]. Yellow River, 2020, 47(S1): 145-146+148.

[10] Chen Yongsheng, Yang Yujun, Li Gang, et al. The effect of alkali free rapid setting agent composite industrial solid waste admixture on the setting time and early strength of cement slurry [J]. China Building Materials Science & Technology, 2025, 34(03): 60-64.

[11] ZHANG Ge, LI Kunpeng, SHI Huawei, et al. Influence mechanism of accelerator on hydration and strength development of shotcrete [J]. Water Resources and Hydropower Engineering, 2024, 55(S1): 449 - 455.

[12] Zha Wenhua, CAI Yukai, Xu Tao, et al. Influence of Admixture Dosage on Mechanical Properties and Impermeability of Coal Gangue Shotcrete [J]. Bulletin of the Chinese ceramic society, 2025, 44(05): 1676-1688.

[13] Wang Yan, Li Yilan, Yang Zifan, et al. Effecet of OPC-SAC Composite Cementitious System on the Properties of Ultra-high Performance Concrete [J]. Materials reports, 2025, 39(02): 94-100.

[14] Wang Lin, Hao Chenchen, Shu Chunxue, et al. Preparation and Hydration Mechanism of High Early Strength Alkali Free and Fluorine Free Liquid Accelerator [J/OL]. Journal of Building Materials, 1-10 [2025-07-14].

[15] LIU Weitao，WU Haifeng，SHEN Jianjun. Based on Box-Behnken method superfine cement grouting material ratio and performance optimization model [J]. Coal Science and Technology, 2024, 52(8): 146−158.

[16] Cheng CAI Development and Experimental Research on Water-Rich Grouting Materials for Coal Gangue Solid Waste [D]. Zhongyuan University of Technology, 2024.

[17] Li Shuai, Chen Zhifeng, Huang Bingyin, et al. Effect of C3A con-tent on hydration and mechanical properties of silicate-sulfoalu minate composite system [J]. Cement, 2024, (08): 80-86.

[18] Yan Ziwei, Liu Li, Sun Jinfeng, et al. Study on the synergistic effect of tricalcium aluminate and calcium carbonate on the early mechanical strength and setting time of portland cement [J]. Chinese journal of the Chinese ceramic bulletin, 2021, 40(05): 1470-1476.

[19] Peng Xinwen. Hydration process of coral powder-portland cement cementitious system and computer simulation [D]. Jiangsu: Nanjing university of aeronautics and astronautics, 2022: 4-29.

[20] Kontoleontos F, Tsakiridis P, Marinos A, et al. Dry-grinded ul-trafine cements hydration. physicochemical and microstructural characterization [J]. Materials research, 2013, 16: 404-416.

[21] Wang Jiahe, Xie Yongjiang, Feng Zhongwei, et al. Effect of accelerator on hydration process of cement in early age [J]. Concrete, 2023, (06): 104-108.

[22] Cheng Cai. Development and experimental research on water-rich grouting materials for coal gangue solid waste [D]. Zhongyuan University of Technology, 2024.